PCCP

Accepted Manuscript

ROYAL SOCIETY OF CHEMISTRY

www.rsc.org/pccp

Chiral Recognition and Atropisomerism in the Sevoflurane Dimer†

Nathan A. Seifert,[a] Cristóbal Pérez,[a,d] Justin L. Neill,[a] Brooks H. Pate,*[a] Montserrat Vallejo-López,[b] Alberto Lesarri,*[b] Emilio J. Cocinero,[c] Fernando Castaño[c]

[a]Department of Chemistry, University of Virginia, McCormick Rd, Charlottesville, VA 22904 (USA)

E-mail: brookspate@virginia.edu, Web: http://faculty.virginia.edu/bpate-lab/

[b]Departamento de Química Física y Química Inorgánica, Facultad de Ciencias, Universidad de Valladolid, 47011 Valladolid (Spain), E-mail: lesarri@qf.uva.es, Web: www.uva.es/lesarri

[c]Departamento de Química Física, Facultad de Ciencia y Tecnología, Universidad del País Vasco (UPV-EHU), Apartado 644, 48080 Bilbao (Spain)

[d]Present address: Max Planck Institute for the Structure and Dynamics of Matter, Luruper Chaussee 149, D-22761 Hamburg (Germany)

†Electronic supplementary information (ESI) available: Additional figures, rotational constants for all isotopic species, ab initio structures, substitution and effective coordinates, structural parameters and full set of measured rotational transitions.

Abstract

We have examined the stereoselectivity of molecular recognition between two molecules of the anesthetic sevoflurane using broadband rotational spectroscopy. The transient axial chirality of sevoflurane is revealed on formation of the dimer, as two different diastereoisomers made of either homo- or heterochiral species are detected in a supersonic jet expansion. The conformational assignment was confirmed by the observation of eighteen different isotopologues in natural abundance (all possible ^{13}C's and two ^{18}O species of the homochiral form). The two clusters are formed in practically equal proportions (1.1:1), probably due to their similar hydrogen bonding topologies. In both clusters the complex is stabilized by a primary C-H···O hydrogen bond, assisted by weak C-H···F interactions. This intermolecular binding regime is characterized by a mixture of electrostatic and dispersive interactions, midway between classical hydrogen bonds and van der Waals clusters.

Introduction

Chiral recognition is the capacity of a molecular probe to provide enantioselectivity, and the chemical basis for chirality separation, induction, transfer or control.[1] Many biological and chemical processes are stereoselective, in particular docking between protein receptors and chiral ligands or interactions between chiral catalysts and substrates in asymmetric synthesis. However, the interest to describe chirality recognition at a molecular level contrasts with the low structural resolution of conventional techniques like FTIR,[2] vibrational circular dichroism (VCD),[3] Raman Optical Activity (ROA),[4] or electronic laser spectroscopies (fluorescence, REMPI, UV/UV and IR/UV double resonance).[5,6] The key to chirality recognition lies in specific combinations of non-bonded interactions, including moderate/weak hydrogen bonding[7] and electrostatic/dispersive forces,[8] which produce stereoselective energetic or kinetic binding differences.[1] Collaborative and cooperative effects, like formation of associative, bifurcated or chained hydrogen bonds, are often relevant to maximize attractive interactions. In some cases aggregation properties depend on competition between different factors, i.e. dispersion and hydrogen bonding. All these forces are ultimately modulated by molecular flexibility and conformational isomerism, not to mention the assistance by water molecules or other binding partners in the physiological medium. For all these reasons obtaining a global model of chirality recognition is challenging, and accurate structural descriptions are usually restricted to small molecular models.[9] In this report we explore how molecular recognition stabilizes transient chirality in the dimer of the general anesthetic sevoflurane, using broadband microwave spectroscopy in a supersonic jet expansion. Microwave spectroscopy is characterized by extreme frequency resolution (kHz), independently resolving all polar species in a gaseous sample. Recent technical advances introducing chirped-pulse excitation have additionally resulted in

order-of magnitude gains in sensitivity and bandwidth,[10] enlarging the scope of this technique to much more complex molecular systems.[11,12] Previous rotational studies have examined the formation of some small chiral intermolecular clusters between neutral molecules, mostly alcohol dimers[13,14,15,16,17] or alcohol clusters involving other chiral or achiral partners.[18,19] These studies have proved useful to observe the formation of homo- and heterochiral diastereoisomers, the conformational preferences, the nature of the chiral discriminating forces (mainly conventional O-H···O hydrogen bonding in aliphatic alcohols), and the performance of alternative techniques and *ab initio* calculations. Chirality discrimination and induction phenomena[1] are particularly noticeable in some of the clusters, but not totally unequivocal due to the low resolution afforded by vibrational techniques. As an example, in the (2,2,2-trifluoroethanol)$_2$ dimer, FTIR, Raman and overtone spectroscopy studies claimed that the dimer would exhibit "quantitative chirality synchronization",[20] since only the homochiral dimer was detected. Conversely, high resolution rotational spectroscopy later established that the heterochiral was also formed in a jet expansion, albeit in lower abundance (10:1).[15] Other dimers show different levels of enantioselectivity. However, the number of clusters for which rotational information is available is still very scarce and the description of chirality recognition is mostly limited to individual cases.

In order to further understand the molecular factors eventually promoting chirality induction or synchronization we decided to examine chiral recognition in larger clusters involving biochemically relevant molecules and weaker interactions (in particular weak hydrogen bonding associated to C-H aliphatic proton donors). The sevoflurane dimer was first selected for several reasons. Sevoflurane is a fluorinated ether used as volatile general anesthetic and its microwave spectrum is known.[21] The molecule is structurally characterized by a single

dominant conformation and noticeable electric dipole moment (μ= 2.270 D), and exhibits several potential binding sites as proton donor (C-H) or acceptor (O and F atoms). A rotational study on sevoflurane···benzene revealed that the C-H bond forms a relatively strong hydrogen bond to the π cloud, assisted by weaker C-H···F interactions.[22] Sevoflurane has no chiral centers, but hindered internal rotation of the terminal fluoromethyl group gives rise to transient axial chirality (R_a, S_a), or atropisomerism.[23] Atropisomerism is known to produce biological stereoselectivity in some natural products and drugs.[24] While the two chiral species cannot be distinguished with conventional spectroscopy techniques, the formation of a bimolecular cluster may stabilize differently one of the two homo- (R_aR_a or S_aS_a) or hetero-chiral (R_aS_a or S_aR_a) species. The IR spectrum of sevoflurane had previously shown blue-shifted vibrational bands tentatively assigned to sevoflurane oligomers,[25] but no structural information on these species was available and stereoisomerism was ignored.

Experimental Section

The chirped-pulse Fourier transform microwave (CP-FTMW) spectrum of sevoflurane dimer was recorded using a CP-FTMW spectrometer at the University of Virginia. Details of this instrumental setup in the context of structure determination have been presented previously,[11] so only details specific to this experiment are given here.

The sample was generated by mixing sevoflurane vapor (brand name Ultane, Abbott Laboratories, 98+%) with ca. 6 atm of neon (GTS Welco) for an approximate concentration of 0.2%, and expanded to form a supersonic jet. The spectrum was acquired by pulsing the sample gas with a backing pressure of ca. 1 atm through 5 pulsed nozzles arranged perpendicularly to the polarization pulse, at a repetition rate of 3.3 Hz. During each valve injection cycle, 4 free

induction decays (FIDs) of the jet-cooled sampled are measured at a total record length of 40 μs which are coherently averaged in the time-domain. The final spectrum consists of a coherent time-domain average of approximately 9.1 million FIDs. All isotopologues measured in this experiment were observed in natural abundance.

Results and discussion

The molecular aggregation of sevoflurane was analyzed in the 2-8 GHz microwave region. The spectrum was comprised of ca. 9,600 rotational transitions with signal-to-noise ratios over 4:1 (1.6 MHz^{-1}), as illustrated in Figure 1. The experiment was assisted by different theoretical calculations for the prediction of the dimer geometries and molecular properties, which combined a molecular mechanics conformational search (MMFFs) with high-level *ab initio* and DFT reoptimization and vibrational frequency calculations (MP2, M06-2X, B3LYP-D3), as in sevoflurane···benzene.[22] Using these initial molecular models, two different species were subsequently detected in the spectrum and identified as the homochiral and heterochiral species of the sevoflurane dimer (ESI† Figures S1 and S2 display 3D rotatable models of the two clusters, with atom labelling in Figures S3 and S4). The detection of a very large set of experimental transitions (700-1000) for each cluster assured the internal consistency of a Watson's[26] semirigid-rotor Hamiltonian fit[27] and led to accurate determination of the rotational constants and some quartic centrifugal distortion parameters. The experimental results are compared with the theoretical predictions in Table 1. The conformational assignment was unequivocally confirmed by the detection of eighteen additional isotopologues in natural abundance. All possible ^{13}C species (ca. 1%) were detected for both homo- and heterochiral clusters, while the two weaker ^{18}O isotopologues (ca. 0.2%) could be observed only for the

homochiral form. Tables S1-S29 (ESI†) collect all the experimental data, *ab initio* structures and relevant information.

The abundance of isotopic data allowed an accurate determination of the cluster structure using both substitution (r_s) and effective (r_0) methods.[28] The experimental (vibrationally-averaged) structures are not directly comparable to the equilibrium *ab initio* structures, but the differences are often within the uncertainty of the derived structural parameters.[11,12] In the sevoflurane dimer the substitution coordinates are in excellent agreement with the MP2 *ab initio* structures in Table S2, with a total (rms) coordinate deviation of 0.067 Å and 0.183 Å, respectively, for the hetero- and homochiral species. The DFT structural predictions were improved compared to the sevoflurane-benzene study by using M06-2X and B3LYP-D3 dispersion-corrected density functionals (DFT structures in Tables S3-S4). The larger deviations for the homochiral dimer are due to imaginary coordinates corresponding to near coincidental positions of several atoms and the inertial axes (Tables S5 and S6 for the homo- and heterochiral dimer, respectively), a well-known issue of the Kraitchman structural method. Figure 2 shows the effective structures of both diastereoisomers and the most relevant intermolecular parameters calculated by a least-squares fit to the moments of inertia,[29] and Table 2 summarizes the essential intermolecular parameters with comparison to the theoretical structures (full experimental coordinates in Tables S7-S9). In this fit all bond parameters containing purely carbon atoms (and oxygen for the homochiral dimer) have been floated, including an intermolecular connectivity between neighboring perfluoro carbons in each of the sevoflurane subunits. All other internal parameters were constrained to the MP2/6-311++g(d,p) structure. Additionally, a comparison of the effective structure parameters of the two subunits of each dimer to that of bare sevoflurane shows an excellent agreement (rms error of 0.025 Å), which confirms the usual assumption that

the monomer geometry is not distorted upon complexation through moderate/weak hydrogen bond forces. The experimental effective structure is graphically compared to the three theoretical methods used in this work (MP2, M06-2X, B3LYP-D3) in Figures S5 and S6. The structural performance of B3LYP-D3 improves the M06-2X results, though still slightly inferior to MP2.

Special attention was paid to the calculation of spectral intensities in order to estimate conformational abundances and, eventually, a preference for one of the two homo- or heterochiral diastereoisomers. The rotational temperature in the jet was first determined by a least-squares fit minimizing the residuals of the intensity ratio between the experimental and predicted values, which resulted in a rotational temperature of 1.32(24) K (including transitions from both disastereoisomers). Since the intensity profile of the rotational spectrum increases with the square of the electric dipole moment, errors in the relative proportions of the theoretical dipole components may cause some uncertainties. To mitigate this, only the common μ_a-type transitions were used, including all assigned transitions with $K_a \leq 20$. The experimental intensity ratio between the homochiral and the heterochiral dimers was then estimated as 1.3 : 1. Assuming the difference in entropy is negligible between the two dimers, this value is in fair agreement with the MP2 counterpoise-corrected energy difference of 22.9 cm^{-1}, which corresponds to a statistical mixture of 1.12 : 1 at 298 K.

The structural data obtained for the sevoflurane dimer confirms that the cluster is held together by a combination of weak hydrogen bonds, with both C-H···F and C-H···O intermolecular linkages. The primary hydrogen bond operates through the isopropyl C-H bond of one of the monomer subunits, acting as proton donor to the oxygen atom in the second monomer. Comparable C-H···F interactions are also found in between the hydrogen in the acceptor's fluoromethoxy group that points closest to the donor fluorines. The r_0-determined C-H···F

linkages range from 2.42(3) Å to 2.86(3) Å, which fall on both sides of the average C-H···F distance of 2.6(1) Å detected in crystallographic studies.[30] The ∠CH···F bonding angles range from ca. 120° in the acceptor fluoromethoxy linkages, to 143° in those containing the donor isopropyl hydrogen. The average angle seen in crystallographic studies falls again somewhere in between (135°). Comparatively, the C-H···O bonding distance and angle seen in both the hetero and homochiral dimers exhibit values of 2.22(5) Å / 146° and 2.44(2) Å / 151(1)°,[31,32] respectively (vs. 2.401(16) Å in sevoflurane···benzene[22]). These values fall in line with the typical C-H···O interaction in crystallographic studies, with typical mean interaction distances of 2.4 Å and angles of 140°.[30]

Since the only significant contributor to an energetic difference between the diastereomers would be found in the intermolecular binding potential, a zeroth-order symmetry adapted perturbation theory (SAPT) calculation[33] was performed to decompose the energetic contributions to the intermolecular binding forces. This calculation used the SAPT(0)/jun-cc-pVDZ[34] level of theory, available in the Psi4 electronic structure package[35] (applied to the B3LYP-D3/6-311++g(d,p) optimized structure). At this level of theory, the total SAPT0 binding energy difference is 6.8 cm^{-1}. Recent benchmark studies of non-covalent interactions suggest that the mean absolute error (MAE) on counterpoise-corrected (cp) binding energy calculations using a Dunning triple-ζ (aug-cc-pVTZ) basis set is 0.126 kcal/mol (44 cm^{-1}),[36] which acts as a lower bound for our determination as the counterpoise-corrected calculations. In this study we used older generation triple-ζ Pople basis set to reduce the computational costs. However, assuming similar benchmark errors, the SAPT(0)/jun-cc-pVDZ binding energy value of 6.8 cm^{-1} is well within the error bounds of the counterpoise-corrected MP2/6-311++g(d,p) value of 22.9 cm^{-1}.

We finally compared quantitatively the intermolecular bonding characteristics in the sevoflurane dimers with related sevoflurane clusters using the SAPT(0) energy decomposition, with the results tabulated in Table 3. Comparison of the SAPT(0) results for both dimers with those of the sevoflurane···benzene complex reveal similar characteristics between both types of complexes. In particular, the total binding energies are very close (-5.97 kcal mol^{-1} for the benzene-containing complex). Like sevoflurane···benzene, the sevoflurane dimer exhibits an intermediate mix of electrostatic and dispersive interactions (less important in the sevoflurane dimer), consistent with the bond distance/angle analysis presented previously. In this regime, the intermolecular binding between sevoflurane monomers falls between the energetic characteristics of a classical hydrogen bond such as the water dimer and that of a dispersion-dominated interaction such as that in benzene···methane. The sevoflurane···H_2O complex has a different C-H···O interaction motif than the sevoflurane dimer. The water-containing complex has an intermolecular binding that is largely electrostatic in character and the C-H···O linkage is much shorter (2.13 Å) and more linear (162°), as reflected in the dominant ΔE_{elst} term from the SAPT(0) analysis.

Conclusions

We have detected and fully characterized the two homo- and heterochiral dimers originated by the transient axial chirality of sevoflurane. The combination of a large set of rotational data from the parent and eighteen different isotopologues together with comprehensive *ab initio* calculations fully specified the molecular structure, conformational abundances and intermolecular binding effects, providing unprecedented details compared to previous molecular studies of weakly-bound intermolecular complexes. No chiral selectivity is observed in the

dimer, as the two homo- and heterochiral diastereoisomers are formed in practically equal (1.1:1) proportions. The similar topology of the hydrogen bonds in the two diastereoisomers, based on a primary C-H···O link assisted by weaker C-H···F contacts, is probably on the origin of this similarity. Other molecular studies of chiral recognition have based the stereoselective preferences in the dissymmetry of the hydrogen bond interactions on exchange of the *R* and *S* species, which are favored by the presence of floppy groups and competing binding sites. This situation is avoided in sevoflurane, dominated by a single most stable conformation. In consequence, further search of molecular origins of enantioselectivity should probably rely on appropriate combinations of weak intramolecular interactions and molecular flexibility. The contribution of dispersive forces to the primary C-H···O hydrogen bond is significant, emphasizing the difficulty to correctly describe the binding properties of the dimer. For these reasons the combination of experimental rotational data with ab initio calculations stands out as a unique tool for an accurate description of weakly bound intermolecular complexes. At the same time, the considerable molecular size of the sevoflurane dimer, one of the largest ever attempted with rotational methods, illustrates the potential of the new chirped-pulse excitation techniques in Structural Chemistry.

Acknowledgements

The authors from the University of Virginia acknowledge funding support from the NSF Major Research Instrumentation program (CHE-0960074). M.V.-L., A.L., E.J.C. and F. C thank the MICINN and MINECO (CTQ-2011-22923, CTQ-2012-39132), the Basque government (IT520-10) and the UPV/EHU (UFI11/23) for funds. M.V.-L. and E.J.C. acknowledge a Ph.D. grant and

a “Ramón y Cajal” contract, respectively. Computational resources of the UPV-EHU were used in this work.

Notes and references

1 a) A. Zehnacker, M. A. Suhm, *Angew. Chem. Int. Ed*. 2008, **47**, 6970. b) A. Zehnacker (Ed.), *Chiral Recognition in the Gas-Phase*, CRC Press: Boca Raton, FL, 2010.
2 M. Albrecht, J. Will, M. A. Suhm, *Angew. Chem. Int. Ed*. 2010, **49**, 6203.
3 L. A. Nafie, *Nat. Prod. Comm*. 2008, **3**, 451.
4 L. D. Barron, F. Zhu, L. Hecht, G. E. Tranter, N. W. Isaacs, *J. Mol. Struct.* 2007, **7**, 834–836.
5 a) D. Scuderi, K. L. Barbu-Debus, A. Zehnacker, *Phys. Chem. Chem. Phys*. 2011, **13**, 17916. b) M. Albrecht, A. Borba, K. Le Barbu-Debus, B. Dittrich, R. Fausto, S. Grimme, A. Mahjoub, M. Nedić, U. Schmitt, L. Schrader, M. A. Suhm, A. Zehnacker-Rentien, J. Zischanga, *New. J. Chem.* 2010, **34**, 1266.
6 J.-P. Schermann, *Spectroscopy and Modelling of Biomolecular Building Blocks*, Elesevier, Amsterdam 2008.
7 a) G. R. Desiraju, T. Steiner, *The weak Hydrogen Bond in Structural Chemistry and Biology*, International Union of Crystallography – Oxford Univ. Press, New York, 2001. b) T. Steiner, *Angew. Chem. Int. Ed*. 2002, **41**, 48.
8 P. Hobza, K. Müller-Dethlefs, *Non-Covalent Interactions, Theory and Experiment*, RSC Publishing, Cambridge, 2010.
9 A. Zehnacker, *Int. Rev. Phys. Chem.* 2014, **33**, 151.
10 a) J.-U. Grabow, "Fourier Transform Microwave Spectroscopy: Measurement and Instrumentation", in *Handbook of High Resolution Spectroscopy* (Ed.: Quack, M.; Merkt, F.), Wiley: New York, 2011, pp. 723-800. b) S. T. Shipman, B. H. Pate, "New Techniques in Microwave Spectroscopy", ibid. pp. 801- 828. c) W. Caminati, "Microwave Spectroscopy of Large Molecules and Molecular Complexes", ibid. pp. 829-852.
11 C. Pérez, S. Lobsiger, N. A. Seifert, D. P. Zaleski, B. Temelso, G. C. Shields, Z. Kisiel, B. H. Pate, *Chem. Phys. Lett.* 2013, **571**, 1.
12 C. Pérez, D. P. Zaleski, N. A. Seifert, B. Temelso, G. C. Shields, Z. Kisiel, B. H. Pate, *Angew. Chem. Int. Ed*. 2014, **53**, 14368.
13 J. P. I. Hearn, R. V. Cobley, B. J. Howard, *J. Chem. Phys.* 2005, **123**, 134234.
14 X. Liu, N. Borho, Y. Xu, *Chem. Eur. J.* 2009, **15**, 270.
15 J. Thomas, Y. Xu, J. *Phys. Chem. Lett*. 2014, **5**, 1850.
16 M. S. Snow, B. J. Howard, L. Evangelisti, W. Caminati, *J. Phys. Chem. A* 2011, **115**, 47.
17 A. M. King, B. J. Howard, *Chem. Phys. Lett.* 2001, **348**, 343.
18 N. Borho, Y. Xu, *Angew. Chem. Int. Ed*. 2007, **46**, 2276.
19 J. Thomas, W. Jäger, Y. Xu, *Angew. Chem. Int. Ed*. 2014, **126**, 7405.
20 a) T. Scharge, T. Häber, M. A. Suhm, *Phys. Chem. Chem. Phys.* 2006, **8**, 4664. b) a) T. Scharge, C. Cezard, P. Zielke, A. Schultz, C. Emmeluth, M. A. Suhm, *Phys. Chem. Chem. Phys.* 2007, **9**, 4472. c) T. Scharge, D. Luckhaus, M. A. Suhm, *Chem. Phys.* 2008, **346**, 467.
21 A. Lesarri, A. Vega-Toribio, R. D. Suenram, D. J. Brugh, J.-U. Grabow, *Phys. Chem. Chem. Phys.* 2010, **12**, 9624.
22 N. A. Seifert, D. Zaleski, C. Pérez, J. L. Neill, B. H. Pate, M. Vallejo-López, A. Lesarri, E. J. Cocinero, F. Castaño, I. Kleiner, *Angew. Chem. Int. Ed*. 2014, **53**, 3210.
23 M. Oki, "Recent Advances in Atropisomerism", in *Topics in Stereochemistry*, vol. 14, chap. 1, Wiley, 1983.
24 A. Zask, J. Murphy, G. A. Ellestad, *Chirality* 2013, **25**, 265.
25 J. J. J. Dom, B. J. van der Veken, B. Michielsen, S. Jacobs, Z. Xue, S. Hesse, H.-M. Loritz, M. A. Suhm, W. A. Herrebout, *Phys. Chem. Chem. Phys*. 2011, **13**, 14142.
26 J. K. G. Watson, "Aspects of Quartic and Sextic Centrifugal Effects on Rotational Energy Levels", in *Vibrational Spectra and Structure*, Vol. 6, Chap. 1, Elsevier: Amsterdam, 1977.
27 H. M. Pickett, *J. Mol. Spectrosc.* 1991, **148**, 371
28 H. D. Rudolph, J. Demaison, "Determination of the Structural Parameters from the Inertial Moments", in *Equilibrium Molecular Structures* (Eds.: J. Demaison, J. E: Boggs, A. G. Császár), CRC Press, Boca Raton (FL), 2010, and references therein.
29 Program STRFIT: Z. Kisiel, *J. Mol. Spectrosc.* 2003, **218**, 58.
30 H.-J. Schneider, *Chem. Sci.* 2012, **3**, 1381.
31 a) G. R. Desiraju, *J. Chem. Soc. Chem. Commun.* 1990, 454. b) G. R. Desiraju, *Acc. Chem. Res.* 1996, **29**, 441.
32 Y. Gu, T. Kar, S. Scheiner, S. *J. Am. Chem. Soc.* 1999, **121**, 9411.
33 B. Jeziorski, R. Moszynski, K. Szalewicz, *Chem. Rev.* 1994, **94**, 1887
34 T. M. Parker, L. A. Burns, R. M. Parrish, A. G. Ryno, C. D. Sherrill, *J. Chem. Phys.* 2014, **140**, 094106

35 J. M. Turney, A. C. Simmonett, R. M. Parrish, E. G. Hohenstein, F. A. Evangelista, J. T. Fermann, B. J. Mintz, L. A. Burns, J. J. Wilke, M. L. Abrams, N. J. Russ, M. L. Leininger, C. L. Janssen, E. T. Seidl, W. D. Allen, H. F. Schaefer, R. A. King, E. F. Valeev, C. D. Sherrill, T. D. Crawford, *Wiley Interdiscip. Rev. Comput. Mol. Sci.* 2012, **2**, 556.
36 L. Goerigk, S. Grimme, *Phys. Chem. Chem. Phys.* 2011, **13**, 6670.

FIGURE CAPTIONS

Figure 1. The broadband MW spectrum of the sevoflurane dimer. The top trace shows a 2 GHz spectral section showing the *J*=6 to *J*=12 series transitions for the dimer. The bottom panel illustrates typical μ_a-type progressions for the two homo and heterochiral species. The experimental traces are compared with simulations using the derived rotational parameters. The dynamic range of the top spectrum was truncated to show the intensity region relevant to the dimer. In this experiment neon was used as carrier gas.

(See file Figure_1.tif)

Figure 2. The effective (r_0) experimental structures derived for the heterochiral (left) and homochiral (right) species of the sevoflurane dimer.

(See file Figure_2.tif)

Table 1. Rotational parameters for the homo- and heterochiral diastereoisomers of the sevoflurane dimer, and comparison with the theoretical predictions.

Homochiral					
	Experimental		**MP2**	**M06-2X**	**B3LYP-D3**
	CP-FTMW			*6-311++g(d,p)*	
A (MHz)[a]	307.789308(39)[b]	A (MHz)[a]	308.11 (0.15%)[c]	314.05 (2.0%)	304.78 (0.99%)
B	172.119904(23)	B	181.76 (3.1%)	185.89 (4.5%)	176.89 (2.7%)
C	168.437022(23)	C	172.83 (1.4%)	182.49 (4.6%)	173.07 (2.7%)
Δ_J (kHz)	0.011420(29)	Δ_J (kHz)	0.00616	0.0224	0.0185[d]
Δ_{JK}	0.029193(43)	Δ_{JK}	0.0185	0.0340	0.0220
Δ_K	-0.035955(67)	Δ_K	-0.0153	-0.0283	-0.0217
$(\mu_a/\mu_b)^2$	16.	$(\mu_a/\mu_b)^2$	11.	2.86	2.92
$(\mu_a/\mu_c)^2$	0.3	$(\mu_a/\mu_c)^2$	0.33	0.35	0.34
		μ_a (D)	-1.86	-1.86	-1.71
N_{lines}	1051	μ_b	0.55	1.10	1.00
RMS (kHz)	8.19	μ_c	3.26	3.15	2.95
		μ_{total}	3.79	3.82	3.55
		ΔE^{CP} (cm^{-1})	0	0	0
Heterochiral					
	Experimental		**MP2**	**M06-2X**	**B3LYP-D3**
	CP-FTMW			*6-311++g(d,p)*	
A (MHz)	304.70027(32)	A (MHz)[a]	306.56 (0.59%)	309.30 (1.5%)	301.15 (1.2%)
B	175.56391(12)	B	183.87 (4.7%)	188.37 (7.3%)	179.12 (2.0%)
C	167.25459(13)	C	174.85 (4.5%)	177.53 (6.1%)	171.40 (2.4%)
Δ_J (kHz)	0.00850(24)	Δ_J (kHz)	0.00548	0.0110	0.0122
Δ_{JK}	0.04428(62)	Δ_{JK}	0.0271	0.0429	0.0794
Δ_K	0.0487(13)	Δ_K	0.0247	0.0349	0.0712
$(\mu_a/\mu_b)^2$	3.2	$(\mu_a/\mu_b)^2$	2.2	3.4	1.5
$(\mu_a/\mu_c)^2$	--	$(\mu_a/\mu_c)^2$	> 100	> 100	41.
		μ_a (D)	2.03	2.53	1.67
N_{lines}	726	μ_b	1.36	1.37	1.37
RMS (kHz)	7.25	μ_c	0.02	-0.14	-0.26
		μ_{total}	2.44	2.88	2.17
		ΔE^{CP} (cm^{-1})	22.9	195.0	60.5

[a]Rotational constants (A, B, C), Watson's A-reduced centrifugal distortion constants (Δ_{JK}, Δ_K), number of measured transitions (N) and microwave RMS deviation of the fit. [b]Standard errors in parentheses in units of the last digit. [c]Absolute percent deviations from the experimental rotational constants. [d]Quartic distortion constants associated with B3LYP-D3 were calculated using the B3LYP level of theory.

Table 2. Selected intermolecular parameters of the observed sevoflurane dimers, with comparison to theoretical structures. The parameters used here correlate with those illustrated in Figure 2, and the notation for the linkages are [acceptor atom] ⋯ [donor atom].

Intermolecular distances / Å	Homochiral				Heterochiral			
	r_0	MP2	M06-2X	B3LYP-D3	r_0	MP2	M06-2X	B3LYP-D3
		6-311++g(d,p)				***6-311++g(d,p)***		
[*syn*-perfluoro F] ⋯ H	2.86(3)	2.70	2.48	2.69	2.48(4)	2.50	2.40	2.54
[*anti*-perfluoro F] ⋯ H	2.67(3)	2.49	2.37	2.56	2.75(3)	2.74	2.54	2.86
O ⋯ H	2.44(2)	2.23	2.28	2.28	2.22(5)	2.21	2.20	2.25
[fluoromethoxy H] ⋯ [fluoromethoxy F]	2.58(3)	2.64	2.71	2.62	2.55(3)	2.48	2.35	2.40
[fluoromethoxy H] ⋯ [*syn*-perfluoro F]	2.42(5)	2.54	2.38	2.50	2.66(4)	2.63	2.57	2.59

Intermolecular distances / Å	Homochiral				Heterochiral			
	r0	MP2	M06-2X	B3LYP-D3	r0	MP2	M06-2X	B3LYP-D3
		6-311++g(d,p)				*6-311++g(d,p)*		
[syn-perfluoro F]…H	2.86(3)	2.70	2.48	2.69	2.48(4)	2.50	2.40	2.54
[anti-perfluoro F]…H	2.67(3)	2.49	2.37	2.56	2.75(3)	2.74	2.54	2.86
O … H	2.44(2)	2.23	2.28	2.28	2.22(5)	2.21	2.20	2.25
[fluoromethoxy H] … [fluoromethoxy F]	2.58(3)	2.64	2.71	2.62	2.55(3)	2.48	2.35	2.40
[fluoromethoxy H] … [syn-perfluoro F]	2.42(5)	2.54	2.38	2.50	2.66(4)	2.63	2.57	2.59

Table 3. Energy decompositions (SAPT(0)/jun-cc-pVDZ) for a selection of sevoflurane clusters, together with three benchmark examples for electrostatic-dominated (water dimer), dispersion-dominated (benzene···methane) and mixed (benzene···acetylene) intermolecular interactions. The SAPT(0) interaction energy is a sum of four chemical energies: the electrostatic (Coulombic) energy ΔE_{elst}, the inductive energy ΔE_{ind} (multipole interactions/charge transfer), the quantum mechanical exchange repulsion energy ΔE_{exch}, and the dispersion stabilization energy ΔE_{disp}.

SAPT(0)/jun-cc-pVDZ (kcal mol^{-1})					
Complex	**ΔE_{elst}**	**ΔE_{ind}**	**ΔE_{exch}**	**ΔE_{disp}**	**ΔE_{tot}**
$(sevo)_2$, homochiral	-7.65	-1.76	9.22	-5.86	-6.05
$(sevo)_2$, heterochiral	-7.52	-1.80	8.96	-5.70	-6.06
sevoflurane···benzene	-8.83	-2.50	14.20	-8.84	-5.97
sevoflurane···H_2O	-10.42	-2.03	7.61	-2.37	-7.21
$(H_2O)_2$	-8.84	-2.15	7.03	-1.27	-5.22
benzene···acetylene	-2.90	-1.06	4.34	-3.32	-2.95
benzene···methane	-0.99	-0.30	2.46	-2.24	-1.07

GRAPHICAL ABSTRACT

Chiral Recognition and Atropisomerism in the Sevoflurane Dimer

N. A. Seifert, C. Pérez, J. L. Neill, B. H. Pate, M. Vallejo-López, A. Lesarri, E. J. Cocinero, F. Castaño

The dimer of sevoflurane illustrates molecular recognition between transiently chiral species. Two different homo- and heterochiral clusters are formed in a jet expansion, stabilized by C-H···O hydro-gen bonds and weak C-H···F interacttions. No enantioselectivity is evident in the dimer, as similar hydrogen-bonding topologies are observed in both species.

(See file "TOC_graphic.tif for image)

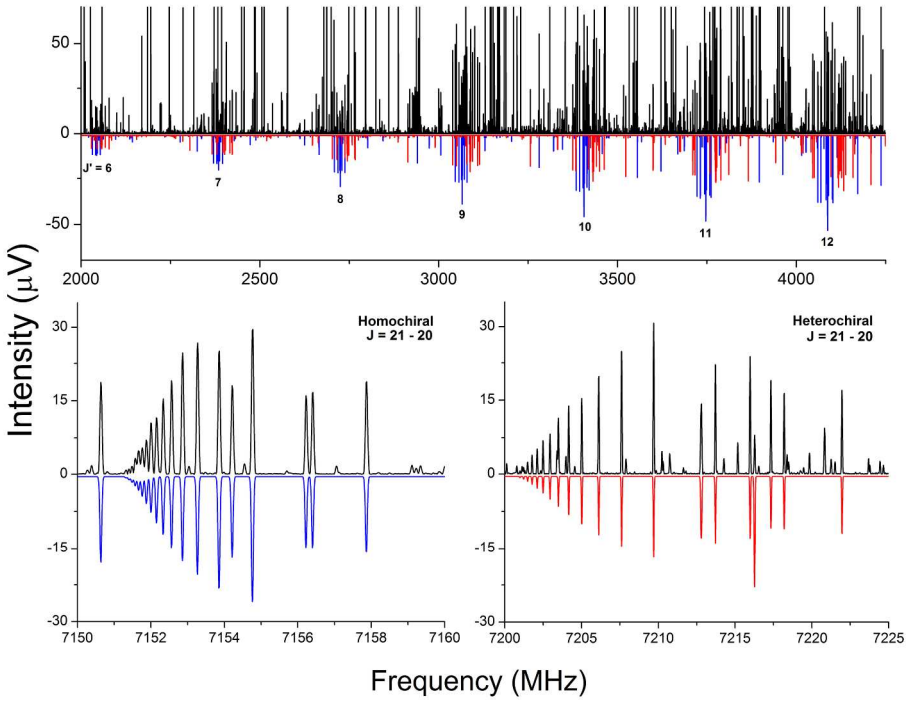

237x187mm (300 x 300 DPI)

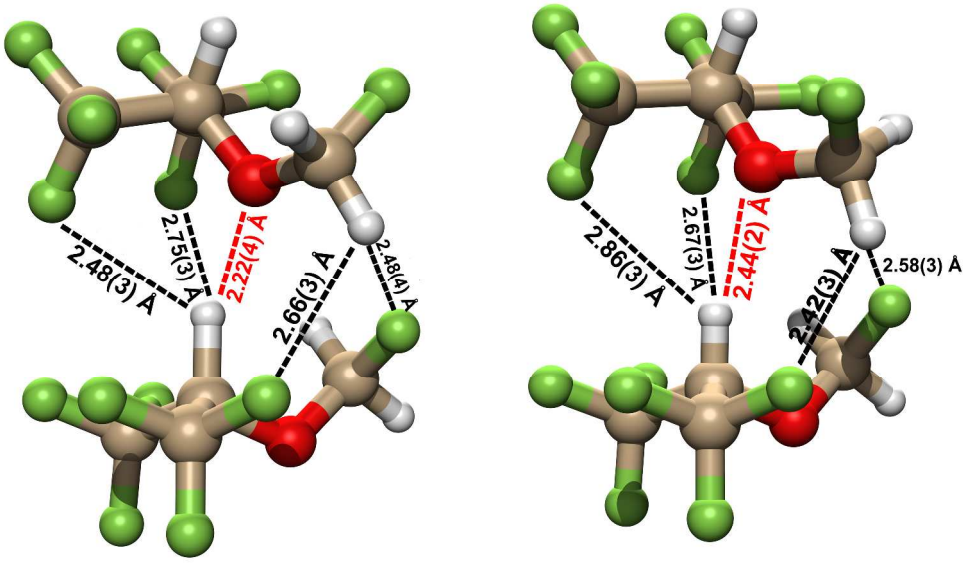

1859x1086mm (72 x 72 DPI)